J. Indian Inst. Sci.
A Multidisciplinary Reviews Journal
ISSN: 0970-4140 Coden-JIISAD

REVIEW ARTICLE

Concerted Pair Motion Due to Double Hydrogen Bonding: The Formic Acid Dimer Case

*Arman Nejad and Martin A. Suhm**

Abstract | Formic acid dimer as the prototypical doubly hydrogen-bonded gas-phase species is discussed from the perspective of the three translational and the three rotational degrees of freedom which are lost when two formic acid molecules form a stable complex. The experimental characterisation of these strongly hindered translations and rotations is reviewed, as are attempts to describe the associated fundamental vibrations, their combinations, and their thermal shifts by different electronic structure calculations and vibrational models. A remarkable match is confirmed for the combination of a CCSD(T)-level harmonic treatment and an MP2-level anharmonic VPT2 correction. Qualitatively correct thermal shifts of the vibrational spectra can be obtained from classical molecular dynamics in CCSD(T)-quality force fields. A detailed analysis suggests that this agreement between experiment and composite theoretical treatment is not strongly affected by fortuitous error cancellation but fully converged variational treatments of the six pair or intermolecular modes and their overtones and combinations in this model system would be welcome.

Keywords: *Hydrogen bond, Anharmonicity, Benchmarking, Formic acid dimer, Vibrations*

1 Introduction

Stable molecules in the gas phase are usually characterised by free and independent translational and rotational motion. It was realised long ago that in some exceptional cases, two or more molecules move in concert for extended periods of time, thus behaving like a single molecule in the gas phase under favourable conditions. This has consequences for the gas density[1] and also for the spectroscopic properties. One of the first examples where such spectroscopic features of molecular aggregation in the gas phase were studied is formic acid (FA).[2] It is a planar pentatomic molecule including the two functional groups which constitute any organic carboxylic acid—an OH group and an adjacent C=O group. The two groups are geometrically arranged in such a way that they can simultaneously form two almost unstrained antiparallel OH···O=C hydrogen bridges, giving rise to a planar (C_{2h}-symmetric) dimer with inversion symmetry (FAD, Fig. 1).

Each monomer brings with it nine vibrational modes, but the dimer generates six additional vibrations which correspond to hindered relative translations and rotations of the paired monomers. All six pair vibrations and even all their binary combinations are lower in frequency than the lowest monomer vibration[3] (for the most abundant HCOOH isotopologue) and this review deals with their nature and exact frequency ν or wavenumber $\tilde{\nu} = \nu/c$, from a computational and experimental perspective. It describes the constraining effect of double hydrogen bonding on molecular motion, at room temperature and at much lower temperatures where it is easier to compare experiment with theoretical predictions. The review also touches on the slow periodic exchange of protons between the two formic acid

Dimer: a pair of molecules or monomers, not necessarily but often identical, which move together for some time, although there is no traditional chemical bond between them.

[1] *Institute of Physical Chemistry, University of Göttingen, Tammannstr. 6, 37077 Göttingen, Germany.*
**msuhm@gwdg.de*

Springer IISc Press

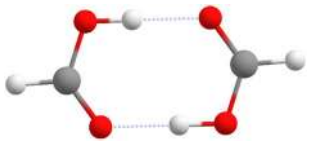

Figure 1: Formic acid dimer (FAD), linking two formic acid molecules together via two rather strong and linear hydrogen bonds (symbolised by blue dashes), optimised at CCSD(T)/aVTZ level.

monomers, which is enabled by these hydrogen bonds and by the symmetry of the complex. This concerted jumping has historically been associated with hydrogen bonding.[4]

Raman-activity: The Raman effect, discovered by the former Director of the Indian Institute of Science C. V. Raman, builds on inelastic light scattering from molecules. Molecular vibrations which change the polarisability can be detected and are called Raman-active, because they modify the frequency of the scattered light.

2 The Six Pair Modes of Formic Acid Dimer

When two non-linear molecules couple their relative motion through intermolecular interactions, there are six degrees of freedom which acquire a restoring force. In the case of two identical planar molecules which form a planar complex, these six vibrational modes can be classified in the following general way (with their formic acid dimer-specific C_{2h} point group representation in parentheses):

Representation: a group theory concept and label which describes how much symmetry is lost during a vibration.

- A dimer stretch modulating the distance of the two monomers (A_g)
- An in-plane shearing motion shifting the two monomers within the common plane (A_g)
- An out-of-plane shearing motion shifting the two molecular planes relative to each other (B_g)
- An out-of-plane bending of the two molecules (A_u)
- An in-plane bending of the two molecules (B_u)
- A twisting of the two molecular planes around a connecting line of the monomers (A_u)

Librations: a special category of vibrations which correspond to hindered rotations or wobbling motions of relatively high frequency.

The first three modes may be viewed as hindered translations, the last three are more similar to hindered rotations of the connected monomers. However, depending on the details of the interactions, there will usually be mixed normal modes involving both translational and rotational character, such that the verbal description above is not universal. Therefore, it is more convenient to use symmetry descriptions which are independent on the limiting behaviour for vanishing interactions, and to combine them with mode designations which encode the small amplitude motion around the minimum energy structure in some pictorial way. In the formic acid dimer case of C_{2h} symmetry, two generating symmetry operations are inversion at the centre and rotation around an axis perpendicular to the dimer plane.

The first three motions listed above conserve the centre of symmetry (subscript g), the last three do not (u). Four of the pair modes conserve the twofold rotational symmetry perpendicular to the molecular plane (symmetry label A), and the other two do not and are, therefore, labelled B. The three u modes generate polarity in the dimer and are thus IR-active. The three g modes modulate the polarisability and are thus Raman-active. Three modes generate non-planar distortions (including either u or B in the label), the other three keep the complex planar (combining either B with u in the label or A with g).

The two in-plane A_g pair modes (denoted ν_8 and ν_9 for formic acid dimer in a nomenclature which sorts the modes according to decreasing frequency within a symmetry block) are close in frequency and may mix intensely, such that it is not so clear which one has more stretching character and which one is more of a shearing or bending nature. The two A_u out-of-plane modes ν_{15} and ν_{16} may also mix, but twisting of the two monomer planes is easier than bending them and, therefore, the mode mixing is less pronounced. The remaining two modes ν_{12} (B_g) and ν_{24} (B_u) are relatively stiff, because both act on the two hydrogen bonds in opposing directions, but these two modes do not mix due to their different symmetry, even if they are close in energy. While they have hydrogen-bond bending and shearing character, like ν_9 and ν_{15}, we qualitatively encode their relative stiffness by calling them somewhat arbitrarily librations (abusing for mnemotechnical reasons the similarity to liberation with respect to attempting to break at least one hydrogen bond), whereas the softer modes ν_9 and ν_{15} are simply denoted bending modes. This yields a twist (A_u), a stretch (A_g), two bends (A_g, A_u), and two librations (B_g, B_u) in a simplified short-hand notation, which we shall keep in the following. It also has the mnemotechnical advantage of locating one bend and one libration each in the infrared and in the Raman spectrum. These four modes can be grouped in two pairs of modes with doubly complementary labels (A_g and B_u as well as A_u and B_g), the so-called Davydov pairs. They combine in-phase (Raman-active) and out-of-phase (IR-active) motion of a similar kind and the stronger the monomers couple with each other, the larger their wavenumber splitting is.

Such Davydov pairs are more easily identified in the monomer modes.[5]

3 Pair Modes and Their Coupling from Experimental Spectra

The experimental characterisation of pair modes of formic acid dimer in the gas phase dates back to as early as 1940[7], because this dimer can be easily prepared under equilibrium conditions around room temperature[8]. However, most of the spectroscopic data obtained under such conditions are strongly distorted,[9, 10], because only about 2% of the dimers are in their lowest vibrational state when they are excited[11]. 98% of the dimers thus already contain some degree of pair mode excitation at room temperature. This makes their spectral signature broad and shifted due to so-called hot transitions. The associated thermal shift of the peak maximum is typically to lower frequency, because excitation weakens the binding between the molecules (Fig. 2). Therefore, the vibrations begin to approach their free rotational and translational limit, which corresponds to much lower frequency than pair vibrations. A good overview of the status about 40 years later is given by Bertie and Michaelian[12]. Due to the associated spectral broadening and shifting, one particular mode (the dimer stretch ν_8) could not be detected at all in these early gas-phase measurements. For the other pair fundamentals, only unreliable, broad band maxima could be obtained, which differ by up to 15% and on average still by more than 6% from current best values. This magnitude of the thermal shift is too large to judge the predictive power of quantum chemical treatments. It indirectly reflects the anharmonicity of pair modes, but it does not allow to analyse this anharmonicity in detail.

By cooling the dimers to much lower temperatures via supersonic jet expansion[13–15] or by spectrally resolving the individual hot vibrational and rotational transitions[13], one can approach the true fundamental vibrational frequencies and also determine some anharmonic couplings. Both are of interest for a rigorous comparison between electronic structure theory and experiment. The alternative cooling mechanism by rare gas matrix isolation[16–22] introduces characteristic matrix embedding shifts on the order of 1–4% for FAD pair modes in Ar[19], which also complicate the comparison to theory[23, 24].

The inversion centre of FAD calls for a combination of infrared and Raman spectroscopy due to the rule of mutual exclusion. The first high-resolution infrared studies of formic acid dimer

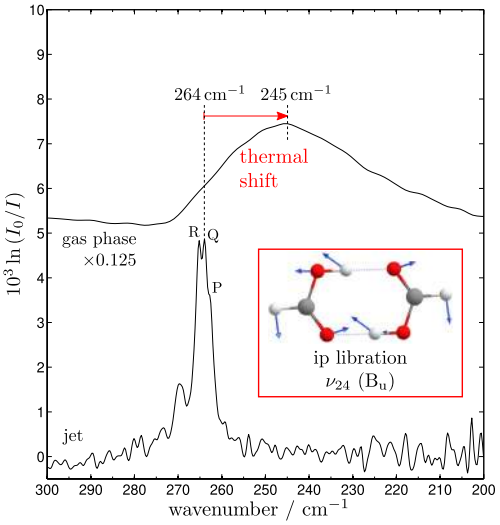

Figure 2: The highest frequency hydrogen-bond vibration ν_{24} for formic acid dimer observed by infrared absorption in a supersonic jet expansion (bottom trace) and in the thermal gas phase (upper trace), where it is downshifted in wavenumber due to thermal effects. Adapted from Ref.[6] with permission from the PCCP Owner Societies.

pair vibrations with resolved hot-band structure were published by Georges et al.[13], about 2 decades after, perhaps, the first such characterisation of a pair mode for a gas-phase complex[25]. Jet-cooled Raman spectra became available in 2007 and unraveled the missing ν_8 mode.[14] Improved Raman spectra were reported in 2009 and also included experimental anharmonicity information from the observation of combination and overtone bands.[26] Since then, the experimental information on Raman-active pair modes was largely complete, whereas the last missing infrared-active fundamental band centre from supersonic jet infrared spectroscopy was reported in 2012 and enabled the calculation of vibrational partition functions.[11] These reliable experimental fundamental transitions and selected experimental anharmonic coupling constants[11, 13, 26] form the basis of the present analysis of capabilities and limitations of electronic structure and vibrational treatments for such hydrogen-bond modes. Eight decades after the pioneering spectroscopy work[7] and four decades after the comprehensive survey over thermally shifted and broadened spectra[12], the present contribution describes this important benchmarking step for the simplest organic dimer with two equivalent hydrogen bonds, building on a large number of now available computational data.

Thermal shift: In spectroscopy, increasing temperature causes increasing amounts of spectral transitions to start from thermally excited levels, thus probing anharmonicity and distorting the low-resolution spectral envelope.

Supersonic jet: an experimental tool to deeply cool molecules translationally and rotationally by adiabatic gas expansion without leading to macroscopic condensation.

Matrix embedding: an experimental technique where molecules and molecular complexes are shock-frozen together with an excess of inert atoms or small molecules, to be studied for extended periods.

Rule of mutual exclusion: vibrations in a molecule with inversion centre cannot be infrared- and Raman-active at the same time.

Benchmarking: a popular and important activity (also) in science, where one picks a prototypical reference system and establishes a (hopefully experimental) reference value for some measurable quantity. Others are then invited to reproduce this benchmark as well as possible. It is important to have several independent benchmarks to avoid fortuitous success and it is important that the reference value is well secured to avoid misdirection.

4 Theoretical Models for the Description of the Six Fundamentals

The theoretical description of the six pair modes of formic acid dimer involves two dimensions—the quality of the electronic structure approximation and the approximation employed for the nuclear motion. Due to the comparatively small number of electrons and their limited coupling in FAD, it is nowadays possible to describe the potential energy hypersurface (PES) quite well by solving the Schrödinger equation for electronic motion, at least close to the global minimum structure. One can go far beyond the simplest Hartree-Fock (HF) or mean-field approximation in terms of electron correlation.[27–29] There are even some recent efforts to analytically parameterise the multidimensional potential as a function of all coordinates at such high levels.[30, 31] A rigorous solution of the multidimensional quantum nuclear motion problem is much more challenging, largely due to the highly coupled nature of the vibrational degrees of freedom.

Potential energy hypersurface: a multidimensional landscape describing the instantaneous electronic energy as a function of atom positions in a molecule, assuming that nuclei move much slower than electrons.

Therefore, we initially focus on the simplest uncoupled harmonic picture, in which the restoring force is assumed to be strictly proportional to the displacement along each vibrational mode. Then, we use vibrational perturbation theory to include leading anharmonic effects in the pair modes, and we discuss the power and limitations of this and other anharmonic approaches, emphasising the danger of error cancellation between the two separate tasks.

4.1 Harmonic Approximation

The simplest approximation is to assume that the restoring force increases linearly along the normal modes of the molecule, the so-called harmonic approximation. For most pair modes, it is plausible that this force increase will actually soften when the interaction between the monomers weakens with increasing separation, such that one expects the harmonic approximation to overestimate rather than underestimate the frequency of the pair vibrations. We calculated harmonic wavenumbers using increasingly accurate HF, MP2, and CCSD(T) ab initio approximations to the electron correlation together with Dunning's augmented correlation consistent basis sets aug-cc-pVXZ[34, 35], using increasingly accurate double- (X = D), triple- (X = T), and quadruple-ζ (X = Q) basis sets, in part repeating or slightly refining previous work[5, 29, 36, 37] to obtain a consistent and systematic set of data. The values are shown in Table 1, together with appropriate experimental and thus anharmonic reference values[11, 13, 26].

Normal modes: Those patterns of nuclear motion in a molecule which are sinusoidal in time if the restoring force is increasing linearly with the displacement.

Depolarisation: When polarised light is scattered from atoms, it conserves this polarisation, but if it is scattered from molecules, at the same time exciting their vibrations, it may lose some of this polarisation and thus gets depolarised.

Also listed are low-resolution gas-phase values[12] which are distorted by thermal excitation (see Fig. 2) and thus not useful for a direct comparison to the theoretical prediction without such excitation. The very fact that they are not comparable shows that the harmonic approximation cannot be perfect in FAD, because in that approximation, spectral peak positions would not show a thermal evolution at all.

It is rewarding that the highest computational level still provides harmonic wavenumbers which are higher than jet-cooled or high-resolution experiment in all cases, by up to 8%. Thus, the expectation that the harmonic approximation overestimates the stiffness of the pair motion is qualitatively met in each case. Regarding the basis set size dependence, we notice that the harmonic wavenumbers do not significantly change, with absolute deviations below 10 cm^{-1}. Changes with the degree of electron correlation can be larger, up to 64 cm^{-1}.

Comparison of the shape of the normal modes reveals only one pronounced effect. A_u, B_u, and B_g modes are largely unaffected by the inclusion of electron correlation, as can be seen in Fig. 4. This, however, is not the case for the shape of the A_g symmetric stretching mode ν_8. At HF level, it mixes with the bending mode of the same symmetry, thus acquiring significant bending character, whereas MP2 and CCSD(T) normal mode calculations predict a better separation between stretching and bending character. This decoupling is caused by an increase of the energetic separation of the two normal modes ν_8/ν_9 which nearly doubles when moving from HF to MP2 or CCSD(T) (Table 1). From experimental Raman depolarisation measurements (Fig. 3),[26] it is known that the two modes are indeed rather cleanly separated in character. The experimental depolarisation ratio of the lower energy ν_9 mode is large, whereas the higher energy band ν_8 is strongly polarised (low depolarisation ratio), as one would expect from a simple stretching motion between two monomer units. This is reflected in harmonically predicted depolarisation ratios for ν_8 which significantly decrease from HF to MP2 (aVDZ: 0.41 → 0.29, aVTZ: 0.40 → 0.26). The larger the depolarisation value for ν_8 is, the more bending character the stretch acquires. Therefore, the qualitative experimental depolarisation behaviour is captured by MP2 calculations, indicating that harmonic normal mode definitions at MP2 and also CCSD(T) level have the right shape, whereas mode mixing is overestimated by HF calculations. Another, more subtle deficiency of the HF calculations is the relative order of the two B

Table 1: Experimental ($\tilde{\nu}_{exp}$) and calculated harmonic (ω_{harm}) values for the six intermolecular fundamental wavenumbers in cm^{-1} for increasingly improved coverage of electron correlation (HF→MP2→CCSD(T)).

		ω_{harm}										
		HF			MP2			CCSD(T)				
		aVDZ	aVTZ	aVQZ	aVDZ	aVTZ	aVQZ	aVDZ	aVTZ	aVQZ [a]	$\tilde{\nu}_{exp}^{ref}$	$\tilde{\nu}_{exp}^{hot\,b}$
ν_9	A_g	161	159	159	169	169	169	168	168	167	161[26]	137[12]
ν_8	A_g	180	179	178	209	213	212	206	211	209	194[26]	-
ν_{12}	B_g	241	239	238	258	258	259	251	253	255	242[26]	230[12]
ν_{16}	A_u	75	75	75	69	69	71	68	69	72	69.2[13]	68[9, 10, 12]
ν_{15}	A_u	167	169	167	175	179	178	171	176	177	168.5[13]	163[10, 12],164[9]
ν_{24}	B_u	220	218	217	275	283	281	269	277	275	264[11 c]	**245**[6], 248[9, 10, 12]

The harmonic values are relatively insensitive to the basis set size (D→T→Q). The splitting between the two A_g modes ν_8 and ν_9 increases considerably from HF to MP2 or CCSD(T). Even the best harmonic calculation is up to 8% higher than experiment. It is essential to compare to cold or high-resolution spectra (column $\tilde{\nu}_{exp}^{ref}$) as a reference to avoid distortion from thermal excitation

[a] Taken from Ref. [29]

[b] "hot" refers to gas-phase spectra at room temperature, where band maxima are shifted due to thermal effects (Figure 2). Further spectra are reported in Refs. [32, 33]. In the present work, the compilation in Ref. [12] is used as a reference, unless there is a more recent value (in bold, ν_{24})

[c] 268 cm^{-1} from high-resolution measurements in gas phase[13]. We have a slight preference for the jet-cooled low-sresolution value (Fig. 2), because the high-resolution thermal spectra[13] are only partially resolved

symmetry librations. Experiment and correlated calculations agree in locating the u mode (ν_{24}) above the g mode (ν_{12}), whereas the HF sequence is inverted. This does not affect the mode pattern, because there is no harmonic mixing for different symmetry. However, it leads to coincidental agreement with experiment for harmonic ν_{12} and to deviations of more than 40 cm^{-1} for the highest frequency pair mode ν_{24}. This further emphasises that good agreement between experiment and theory may not happen for a good reason whenever two or more factors contribute.

The key remaining question is whether the deviation between the best, i.e., CCSD(T) large basis set harmonic calculations, and experiment of still up to 8% is due to residual deficiencies of the electronic structure calculation or due to anharmonic motion in this moderately floppy dimer. If the latter is the case, one would like to know whether the anharmonicity effects are diagonal, along a normal mode, or off-diagonal, involving a coupling between two or more modes. Even if the net anharmonicity effect is small, it may still be the result of mutually cancelling anharmonic contributions.[38] The next chapter tries to provide computational background for this question.

4.2 Beyond the Harmonic Approximation

Assuming that the harmonic approximation already gives a good zeroth-order description, anharmonicity for each fundamental can be calculated as a small correction using second order perturbation theory (VPT2).[40] This is more likely the case in FAD than, e.g., for the dimer of acetic acid[41], because the methyl group torsion in the latter is periodic with multiple equivalent minima, rather than harmonic. This renders FAD a particularly valuable reference system. Indeed, VPT2 has been applied to FAD repeatedly in the past, using MP2 and the B3LYP functional with different basis set sizes and often combining the anharmonic corrections with higher quality harmonic wavenumbers. B3LYP VPT2 calculations have been performed with 6-31+G(d)[42], 6-311++G(2d,2p)[26], SNSD/T[43], VTZ[44], aVTZ[37, 43], as well as aVTZ and def2-TZVP with dispersion-corrected B3LYP-D3(BJ)[5]. MP2 VPT2 calculations have been performed with 6-31+G*, 6-311+G*[26], 6-311+G(d,p)[45], and aVDZ[29] basis sets.

In VPT2, fundamental transitions $\tilde{\nu}_i$ are calculated as:

$$\tilde{\nu}_i = \omega_{\mathrm{harm},i} + 2x_{i,i} + \frac{1}{2}\sum_{j\neq i} x_{i,j}, \qquad (1)$$

where $x_{i,i}$ is the diagonal anharmonicity constant along normal mode i and $x_{i,j}$ describes off-diagonal anharmonicity which introduces binary coupling between two different normal modes i and j.

VPT2: vibrational energy levels are calculated by considering perturbations from all other modes, which should not come too close to the mode of interest.

Harmonic mixing: If two normal modes with the same symmetry label get close in energy, they may acquire a mixed character and the degree of mixing depends on fine details of the PES. If they have different symmetry labels, such mixing of the vibrational character is not possible.

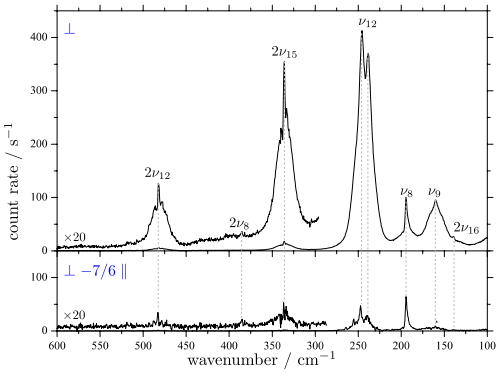

Figure 3: Raman scattering spectrum of FAD in He (≈ 0.7%) with the polarisation of the incident laser perpendicular with respect to the scattering plane (⊥, top) and residual after subtracting 7/6 of the spectrum obtained with the laser polarisation parallel to the scattering plane (⊥ −7/6 ∥, bottom). Bands that persist more in the residual spectrum have smaller depolarisation ratios. Adapted from Ref. [26], with the permission of AIP publishing.

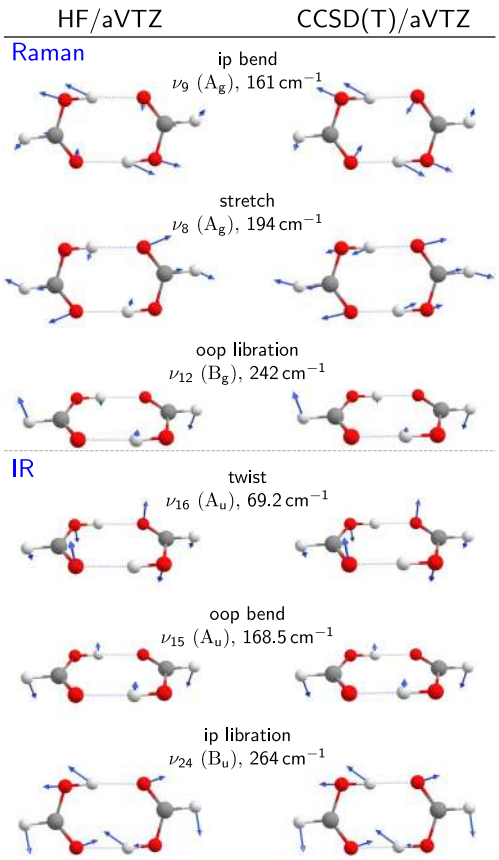

Figure 4: Normal modes for all six intermolecular or pair vibrations of formic acid dimer (FAD) calculated at HF/aVTZ and CCSD(T)/aVTZ level, their short-hand designation, and their experimental fundamental wavenumbers in cm^{-1}, from Refs. [11, 13, 26].

Numerical errors: computer programs have to truncate numbers after a certain number of digits and this leads to errors in computational results which get larger with every operation and in particular numerical differentiation, where one divides through small numbers.

To be able to compare to experiment and to non-perturbational, i.e., variational approaches, we define the anharmonic correction for a fundamental i as the difference between its anharmonic and harmonic wavenumber:

$$\delta_{\mathrm{anh},i} = \tilde{\nu}_i - \omega_{\mathrm{harm},i}. \qquad (2)$$

$\delta_{\mathrm{anh},i}$ cannot be obtained from experiment in an easy and direct way, but our working hypothesis for this section is to assume that the large basis set harmonic CCSD(T) values obtained earlier[29] are close to the true harmonic values, such that their comparison to $\tilde{\nu}^{\mathrm{ref}}_{\mathrm{exp},i}$ yields an experimental estimate:

$$\delta^{\mathrm{exp}}_{\mathrm{anh},i} \approx \tilde{\nu}^{\mathrm{ref}}_{\mathrm{exp},i} - \omega_{\mathrm{harm},i}(\mathrm{CCSD(T)/aVQZ}). \qquad (3)$$

First of all, it must be emphasised that VPT2 calculations are more susceptible to numerical errors than harmonic calculations, because they typically rely on numerical higher derivatives of the potential. We estimate the size of this numerical error by starting independent structure optimisations from nine independent equilibrium structures (combination of HF, MP2, and CCSD(T) optimised structures with aVDZ, aVTZ, and aVQZ basis sets). After rounding, this statistical analysis gives rise to the error bars provided in parentheses in Table 2 which are estimated as half of the maximum absolute deviation for each fundamental, respectively. One can see that this numerical noise ranges from 1 to 6 cm^{-1}, which can be larger than the individual anharmonic correction in some cases. This aspect of VPT2 calculations is often overlooked and we recommend multiple independent calculations using tight optimisation criteria with and without symmetry to unravel numerical noise.[46] The remaining noise must be kept in mind when interpreting the VPT2 numbers. Nevertheless, several trends are evident from Table 2. Within error bars, all anharmonic corrections for the six pair vibration fundamentals are negative, but the lowest frequency twist mode is particularly susceptible to such numerical error. Basis set effects are smaller than the statistical error, whereas the anharmonic corrections at MP2 level are typically less negative than those at HF level. They match the discrepancy between the highest level harmonic prediction and the experimental anharmonic fundamentals $\delta^{\mathrm{exp}}_{\mathrm{anh}}$ significantly better, in some cases even within numerical error bar. This is visualised in Fig. 5, where the size of the coloured bars represents the deviation of the anharmonic corrections from the harmonic CCSD(T) mismatch with respect to experiment. It provides

quite compelling evidence that the harmonic CCSD(T) results are very close to the true harmonic wavenumbers if the VPT2 calculations can be trusted in this case. Furthermore, it suggests that MP2 anharmonic corrections are, in most cases, more accurate than HF anharmonic corrections. A composite method which combines harmonic CCSD(T) fundamental wavenumbers with MP2 anharmonicity corrections is suggested to be essentially exact for the pair modes, within the numerical accuracy of our VPT2 calculations. This remarkable result has been obtained for the first time in a study on the dissociation energy of FAD with respect to two monomers by Miliordos and Xantheas[29], which also matches the currently best experimental value[11] exceptionally well. A simultaneous match of spectroscopic and thermodynamic data may be taken as indication for the smallness of accidental error compensation, whereas a preceding, rather similar study[37] obtained a good match due to the cancellation of two errors.

The success of MP2 VPT2 calculations for FAD pair modes must be contrasted to recent results using the fundamentally superior variational configuration interaction (VCI) method [39], which are also included in Fig. 5. They systematically overshoot the experimental fundamentals, although they are based on a CCSD(T) quality PES. Evidently, this should not be blamed on the underlying full-dimensional semi-global PES[31], but rather on the approximations required for a high-dimensional variational calculation, such as a limited number of modes which are coupled together and a limited basis set. We cannot go into details, but the description of large-amplitude low-frequency modes, even if they are initially as closely harmonic as in the case of FAD, apparently can give rise to problems for a normal coordinate formulation of VCI. Other spectral regions appear to be less susceptible to such limitations[47] and a curvilinear treatment might be indicated[48, 49].

Clearly, VPT2 with an anharmonic MP2 PES offers an attractive way to describe the pair modes of FAD in combination with a high-quality harmonic reference. This was already observed before[26, 29] and the present analysis confirms that the discrepancy to the low temperature or rotationally resolved experiments is essentially within the numerical noise of the perturbation method. This brings us to the next challenge: Is there also a way to model the more easily accessible low-resolution room temperature spectra of FAD?[12]

4.3 Simulating Thermal Shifts

A popular way to obtain anharmonic fundamental frequencies for larger systems is classical molecular dynamics in PES which are either generated on the fly or analytically[50]. This is usually called ab initio molecular dynamics (AIMD), although for reasons of computational effort, the on-the-fly variant typically uses more or less empirically refined density functionals. Due to fundamental deficiencies of density functional theory (DFT) in accurately describing hydrogen bonds, such as overestimated downshifts of hydrogen-bonded stretching modes, the neglect of the quantum character of vibrations is usually blurred in such DFT AIMD simulations. More often than not, the overestimation of harmonic downshifts in DFT is qualitatively compensated by the inability of classical dynamics to sample

VCI: vibrational energy levels are calculated by coupling all states with different excitations together, including closely spaced neighbors.

Classical molecular dynamics: an approximation to molecular vibration in which one pretends that the atoms follow Newton's classical equations of motion and thus ignores quantum effects such as tunneling. This can be acceptable for heavy atom and molecule motion and for harmonic systems (due to the correspondence principle) or high temperatures, but may fail badly for light atoms in anharmonic potentials at low temperatures.

Table 2: Averaged anharmonic corrections (in cm^{-1}) from VPT2 calculations at HF and MP2 level and subtly different optimised structures, computed according to Eq. (2).

		$\delta_{anh} = \tilde{\nu} - \omega_{harm}$				
		HF		MP2		
		aVDZ	aVTZ	aVDZ[a]	aVTZ	δ_{anh}^{exp} [b]
ν_9	A_g	−11(1)	−12(1)	−8(1)	−8(3)	−6
ν_8	A_g	−14(1)	−16(3)	−15(1)	−15(2)	−15
ν_{12}	B_g	−19(2)	−20(2)	−13(1)	−12(3)	−13
ν_{16}	A_u	−3(4)	−3(4)	−2(2)	3(6)	−3
ν_{15}	A_u	−8(3)	−12(5)	−6(2)	−6(4)	−8
ν_{24}	A_u	−18(1)	−20(1)	−12(1)	−10(2)	−11

Errors in the last digit are given in parentheses (see main text for explanations)
[a] Data presented by Miliordos and Xantheas[29] are reproduced within the given error bars
[b] δ_{anh}^{exp} is estimated from "best" available harmonic values [29], according to Eq. (3)

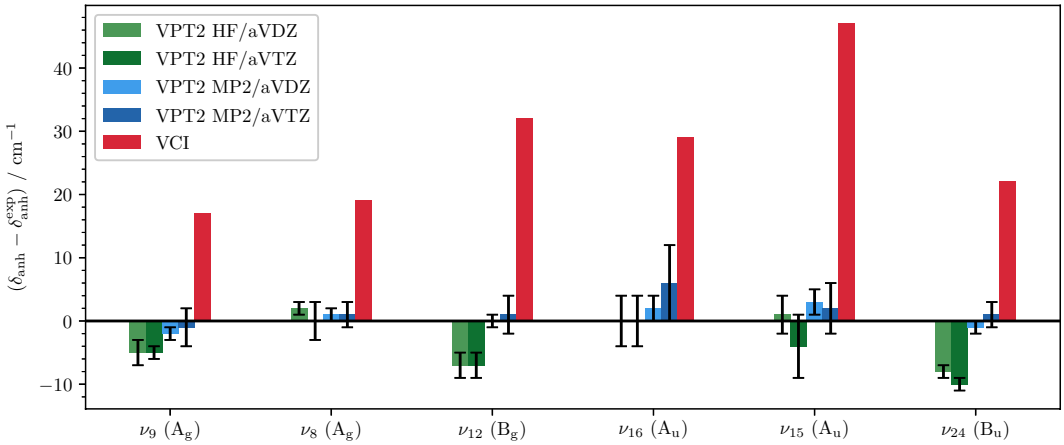

Figure 5: Deviation between calculated (δ_{anh}) and experimental (δ_{anh}^{exp}) anharmonic corrections, estimated according to Eq. (3). VCI data by Qu and Bowman are taken from Table 1 of Ref. [39]. A value of 0 means perfect agreement between theory and experiment, assuming that the harmonic reference to estimate δ_{anh}^{exp} is correct.

the anharmonic region probed by the quantum nature of the hydrogen atom. This frequently provides right answers for the wrong reasons[50,51], whenever high-frequency XH stretching spectra are simulated, because in this case, temperatures of several 1000 K would be needed to sample the relevant fundamental vibrational displacements.

For the low-frequency pair modes which are discussed here, the situation is more comfortable, because the thermal energy at room temperature $kT_{300\,K}$ is much closer to the vibrational energy quantisation $h\nu$. Therefore, a classical molecular dynamics simulation of these modes at room temperature is qualitatively able to sample the relevant anharmonic potential for fundamental excitation. As there is a high-quality full-dimensional PES of FAD [31,39,47], it is instructive to analyse the thermally sampled fundamental wavenumbers obtained by running classical molecular dynamics simulations in it [39]. In Fig. 6, the result of such simulations at 300 K extracted from Table 1 of Ref.[39] is compared not to the experimental fundamental band centres themselves (that would imply that kT is always close to $h\nu$), but rather to the thermal shift of the experimental fundamental vibrations from the best band centre reference, both listed in Table 1. The agreement is qualitatively satisfactory, with the correct sign of the thermal shift being predicted by AIMD(300 K)−AIMD(0 K), where AIMD(0 K) is simply the harmonic normal mode wavenumber. However, the predicted thermal shifts are always smaller than the experimentally observed shifts. One might have expected the opposite, because AIMD(0 K) lacks anharmonicity, whereas $\tilde{\nu}_{exp}^{ref}$ already contains some of that. However, given the crudeness of the classical molecular dynamics approach, the absence of appropriate sampling of the high-frequency modes, and the complexity of hot vibrational spectra, the agreement is quite satisfactory. It would be interesting to compute for each mode the required temperature to match the experimental thermal shift of the band maximum.

5 Beyond Fundamentals—Combined and Overtone Excitations

After having shown that a combination of high-quality electronic structure calculations and vibrational perturbation theory provides a rather satisfactory description of the fundamental excitation of pair modes in formic acid dimer within numerical accuracy and that even thermal shifts can be modelled reasonably well, one has to ask whether this is to some extent fortuitous. For this purpose, it is worthwhile to dissect the total anharmonic contributions further, to check for potential coincidental error compensation. Rewardingly, some combination and overtone bands of pair fundamentals are available from high-resolution or jet-cooled experiments[11,13,26]. If one measures such a combined $i+j$ (or double $i+i$) excitation and subtracts the values for the individual fundamental excitations, one arrives at the off-diagonal (diagonal) terms $x_{i,j}$ ($x_{i,i}$) contained in Eq. (1). The resulting expressions

$$x_{i,i} = \tilde{\nu}_{i+i}/2 - \tilde{\nu}_i \tag{4}$$

$$x_{i,j} = \tilde{\nu}_{i+j} - \tilde{\nu}_i - \tilde{\nu}_j \tag{5}$$

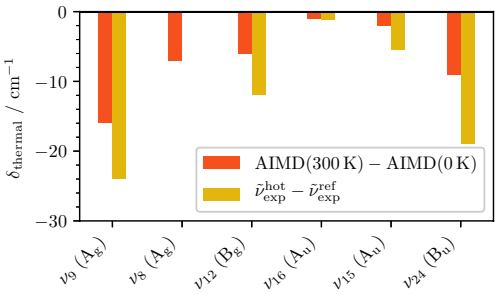

Figure 6: Thermal shifts $\tilde{\nu}^{\text{hot}}_{\text{exp}} - \tilde{\nu}^{\text{ref}}_{\text{exp}}$ observed for the pair modes of FAD from Table 1 in comparison to predictions from a classical molecular dynamics simulation[39] in a high-quality potential energy hypersurface (AIMD(300 K)−AIMD(0 K)). The simulation underestimates the experimental shifts, in particular for the librations, but the qualitative trends are reasonable.

can be applied in all cases where reasonably reliable spectroscopic data are available (Fig. 7; Table 3). Agreement between theory and experiment is indeed very satisfactory at this individual coupling level within the experimental and numerical error bars. Although there is always a risk of misassignment in particular for the low-resolution jet data, which involve very weak transitions, the close correlation between theory and experiment suggests that error compensation among the $x_{i,j}$ is not a major issue. Two things are noteworthy in this context. A pronounced tendency for negative anharmonicity corrections is, perhaps, not so surprising if one remembers that these are pair modes which correlate with translations and rotations in the limit of high vibrational excitation. However, it strongly indicates that there can be little error compensation for the anharmonicity in the fundamentals, because that would require both negative and positive contributions. Furthermore, the basis set dependence and also the electron correlation effects are very modest. This further validates popular composite approaches[29] where the harmonic predictions are carried to the highest affordable electronic structure level, whereas the anharmonic corrections can be dealt with at a lower level of theory. It also explains why the AIMD simulations give the right sign of the spectral shift upon thermal excitation, although not the correct size. There is so far no experimental evidence for significant positive diagonal or off-diagonal contributions which might cancel the negative ones, although it must be emphasised that the experimental characterisation is far from complete.

6 A Much Slower Concerted Motion—Proton Tunneling

While the fundamental intermolecular vibrations of the formic acid dimer discussed so far happen on a 0.1–0.5 ps time scale, there is one prominent quantised motion in FAD which is four orders of magnitude slower and thus proceeds on the low ns time scale. This is the concerted exchange of two protons between the two acid monomers (Fig. 8), by tunneling through a barrier which is greatly attenuated compared to bond breaking, but still rather high.[53] Understandably, this prototypical proton exchange has met a lot of interest and numerous attempts to compute its time scale, including early work by Meyer et al.[54], Chang et al.[55], Shida et al.[56], and more recent work by Liedl et al.[57,58], Luckhaus[53,59], Nakamura et al.[60,61], Došlić et al.[62–64], Sibert III et al.[30,65,66], Bowman et al.[31,67], Siebrand et al.[68–71], Ivanov et al.[72], and Richardson[73].

Tunneling: a quantum phenomenon, where light particles, here the two acidic protons, disappear in one place and reappear in an equivalent one, without much likelihood to catch them in between.

There have been key experiments to determine this periodic motion from high-resolution spectroscopy. Spectroscopy yields a splitting $\Delta\nu$, which in a two-level system is related to the full tunneling period Δt by $\Delta t = 1/\Delta\nu$, similar to the relationship for fundamental frequencies. The standard way of measuring this splitting, namely rotational spectroscopy, was hampered until recently by the lack of a dipole moment in the formic acid dimer. Unsymmetric isotope substitution helps to generate such a dipole moment, and very recently, it has been used to experimentally determine the ground-state exchange process directly.[74] The alternative in the absence of a dipole moment was and is high-resolution vibrational spectroscopy through combination differences. This was pioneered for formic acid dimer by the Havenith group[52,75,76] and followed up by the group of Duan[77,78]. Figure 8 shows the evolution of experimental assignments for tunneling periods obtained from tunneling splittings in the ground state of formic acid dimer over the last 2 decades. Values which involve one or two D atoms instead of H at the carbon atoms are included, because their effect on the tunneling process is comparatively small compared to the evolution of the best value with time. One can see how the best full back-and-forth period Δt of the experimental periodic proton tunneling process has evolved over time and is now seen to amount to 3 ns, whereas it was long thought to be close to 2 ns. Because of the high sensitivity of this value to the detailed experimental analysis of rotation–tunneling coupling[77,78], it will continue to challenge theory and experiment, if a $\approx$ 1% level of agreement like in the fundamental intermolecular

Tunneling period: The total time which it takes for a light particle to fully disappear from one position and to reappear in an equivalent one which is separated by a barrier, and then to move back to the original position in the same disappearing/appearing fashion.

modes is aimed at. The dependence of this tunneling process on vibrational excitation is of particular interest[76] and will at some stage compete with ring-opening isomerisation[79].

7 Future Challenges

This review has strongly focused on the intermolecular or pair modes of the main isotopologue of cyclic FAD and has demonstrated a remarkable match between theory and experiment. It has not yet explored the power of isotope substitution[80], which provides valuable independent checks from the experimental side and sometimes even surprising phenomena such as counterintuitive isotope effects[14] which have to be modelled by quantum treatments of the nuclear dynamics. Alternatives to the relatively insensitive linear FTIR and Raman spectroscopy for jet-cooled species[81] have to be further developed in different spectral ranges, either as linear[15, 82, 83] or as action spectroscopy[84, 85] tools, also extending into different environments[85–89].

When moving up the energy ladder, the success of VPT2 to model the anharmonicity is expected to fade somewhat, as soon as monomer modes become accessible. While the monomer itself is vibrationally rather well understood[90, 91], it contains several strong resonances. Furthermore, the two monomers need to be coupled together and with the pair modes. It is important to build on the good VPT2 performance for the pair modes as test cases for alternative, presumably mostly variational methods[48, 92–94], which reach further up on the energy scale. It may be too ambitious to aim at a quantitative description of the complex coupling pattern in the OH stretching region[36, 41, 95–97], but the more isolated couplings in the monomer fingerprint up to the carbonyl stretching region[81] are waiting to be understood in detail for FAD. Between these carbonyl stretching fundamentals and the OH stretching region, the PES starts to open up for other, metastable isomers[20, 79, 98–103], which need to be characterised. The enormous sensitivity of matrix isolation spectroscopy[104] can also be exploited towards this goal once the subtleties of spectral matrix shifts[23, 24, 96, 105] are better

Table 3: Selection of binary combination, overtone, and hot bands of intermolecular fundamentals in cm^{-1} from jet-cooled and high-resolution spectra, from which the anharmonicity constants in Fig. 7 are obtained, according to Eqs. (4) and (5), together with fundamental transition wavenumbers from Table 1.

Transition		$\tilde{\nu}^{ref}_{exp}$	Transition		$\tilde{\nu}^{ref}_{exp}$
$\nu_9+\nu_9$	A_g	319[26]	$\nu_9+\nu_{12}$	B_g	400[26]
$\nu_8+\nu_8$	A_g	386[26]	$\nu_9+\nu_{24}$	B_u	419[11]
$\nu_{12}+\nu_{12}$	A_g	482[26]	$\nu_8+\nu_{24}$	B_u	451[11]
$\nu_{16}+\nu_{16}$	A_g	139[26]	$\nu_{12}+\nu_{16}$	B_u	311[11]
$\nu_{15}+\nu_{15}$	A_g	336[26]	$\nu_{15}+\nu_{16}-\nu_{16}$ [a]	A_u	167.26[13]
$\nu_{24}+\nu_{24}$	A_g	518[11, 26]			

[a]The off-diagonal constant $x_{i,j}$ is computed from the hot and fundamental transition wavenumbers as $x_{i,j}=\tilde{\nu}_{i+j-j}-\tilde{\nu}_i$

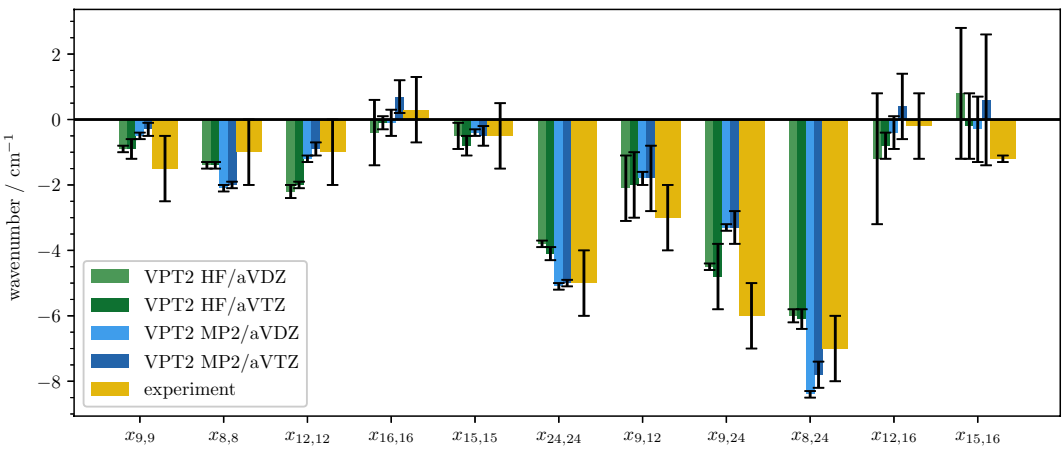

Figure 7: Some diagonal- ($x_{i,i}$) and off-diagonal ($x_{i,j}$) anharmonicity matrix elements for the six intermolecular modes, computed according to Eqs. (4) and (5). The selection is based on reasonably reliable experimental jet-cooled or high-resolution values[11, 13, 26] with roughly estimated error bars, see Table 3. $x_{24,24}$ is particularly tentative[11, 26] and only included for convenience. Numerical VPT2 error bars are rounded up to the first decimal place if $< 0.5\,cm^{-1}$, else to the next full digit.

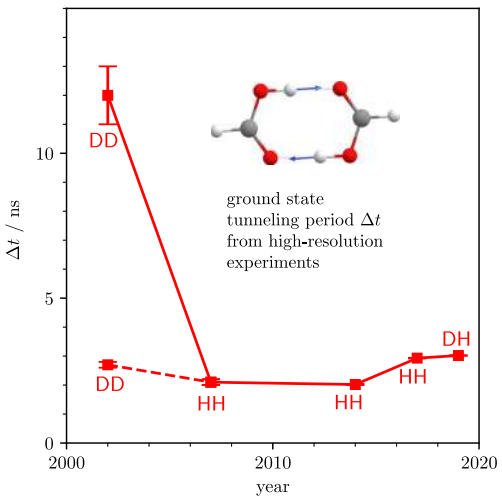

Figure 8: Evolution of the experimental ground-state tunneling period Δt as a function of publication year, including an ambiguity in the first experiment[52]. DD/HH/DH marks the isotope pattern of the two other hydrogens in the CD/CH bond. See text for further details.

understood. For spectral simulations with intensity information, the development of dipole moment[106] and polarisability hypersurfaces would be helpful.

Once the vibrational treatment of FAD is well established and converged, one can also turn back to the electronic structure challenge and use the available data for the benchmarking of conventional and less conventional methods[107] applicable to the quantitative description of double hydrogen-bond potential energy hypersurfaces.

8 Conclusions

We have shown how experiment and theory can be brought together in a systematic way for the six pair or intermolecular modes of the cyclic form of formic acid dimer. Fortuitous error cancellation between electronic structure theory and vibrational treatment could be largely ruled out. This represents a stepping stone from which higher vibrational excitations, different isotopologues, structural isomers, thermal excitation, and increasingly interacting environments for the dimer have to be addressed to complete the challenging benchmarking task for the simplest organic doubly hydrogen-bonded complex in the next decade and beyond. This will require major efforts on the experimental and on the theoretical side, but the reward will be a unique reference point for the correct and quantitative description of double hydrogen bonding and its intriguing dynamics, always aiming at the right answers for the best possible reasons.

Publisher's Note

Springer Nature remains neutral with regard to jurisdictional claims in published maps and institutional affiliations.

Acknowledgements

We greatly acknowledge financial support by the Deutsche Forschungsgemeinschaft (DFG, project numbers 388861488 and 389479699/GRK2455) and thank Katharina A. E. Meyer for valuable discussions. A. Nejad thanks the Fonds der Chemischen Industrie (FCI) for an attractive scholarship.

Frequency calculations were performed with the CFOUR[108] (CCSD(T), all convergence thresholds $= 10^{-9}$, frozen_core = On), and Gaussian09 Rev. E01[109] (Opt = VeryTight, Symmetry = On) program packages, molecular structures visualised with ChemCraft[110], and figures created with Matplotlib[111].

Compliance with Ethical Standards

Conflict of interest

The authors declare that they have no conflict of interest.

Open Access

Received: 10 September 2019 Accepted: 25 October 2019
Published online: 22 November 2019

References

1. Coolidge AS (1928) The vapor density and some other properties of formic acid. J Am Chem Soc 50(8):2166–2178
2. Bonner LG, Hofstadter R (1938) Vibration spectra and molecular structure IV. The infra-red absorption spectra of the double and single molecules of formic acid. J Chem Phys 6(9):531–534

3. Miyazawa T, Pitzer KS (1959) Internal rotation and infrared spectra of formic acid monomer and normal coordinate treatment of out-of-plane vibrations of monomer, dimer, and polymer. J Chem Phys 30(4):1076–1086
4. Herzberg G (1945) Molecular spectra and molecular structure. II. Infrared and Raman spectra of polyatomic molecules. Princeton University, Princeton
5. Meyer KAE, Suhm MA (2018) Vibrational exciton coupling in homo and hetero dimers of carboxylic acids studied by linear infrared and Raman jet spectroscopy. J Chem Phys 149(10):104307
6. Suhm MA, Kollipost F (2013) Femtisecond single-mole infrared spectroscopy of molecular clusters. Phys Chem Chem Phys 15:10702–10721
7. Bonner LG, Kirby-Smith JS (1940) The Raman spectrum of formic acid vapor. Phys Rev 57:1078
8. Wachs T, Borchardt D, Bauer SH (1987) Resolution of spectra of mixtures, applied to gaseous formic acids. Spectrochim Acta Part A 43(7):965–969
9. Carlson GL, Witkowski RE, Fateley WG (1966) Far infrared spectra of dimeric and crystalline formic and acetic acids. Spectrochim Acta 22(6):1117–1123
10. Clague D, Novak A (1970) Far infrared spectra of homogeneous and heterogeneous dimers of some carboxylic acids. J Mol Struct 5(1):149–152
11. Kollipost F, Larsen RW, Domanskaya AV, Nörenberg M, Suhm MA (2012) Communication: the highest frequency hydrogen bond vibration and an experimental value for the dissociation energy of formic acid dimer. J Chem Phys 136(15):151101
12. Bertie JE, Michaelian KH (1982) The Raman spectra of gaseous formic acid -h_2 and -d_2. J Chem Phys 76(2):886–894
13. Georges R, Freytes M, Hurtmans D, Kleiner I, Vander Auwera J, Herman M (2004) Jet-cooled and room temperature FTIR spectra of the dimer of formic acid in the gas phase. Chem Phys 305(1):187–196
14. Zielke P, Suhm MA (2007) Raman jet spectroscopy of formic acid dimers: low frequency vibrational dynamics and beyond. Phys Chem Chem Phys 9:4528–4534
15. Ito F (2007) Jet-cooled infrared spectra of the formic acid dimer by cavity ring-down spectroscopy: Observation of the C–O stretching region and vibrational analysis of the Fermi-triad system. Chem Phys Lett 447(4):202–207
16. Halupka M, Sander W (1998) A simple method for the matrix isolation of monomeric and dimeric carboxylic acids. Spectrochim Acta Part A 54(3):495–500
17. Gantenberg M, Halupka M, Sander W (2000) Dimerization of formic acid—an example of a "noncovalent" reaction mechanism. Chem Eur J 6(10):1865–1869
18. Ito F (2008) Infrared spectra of $(HCOOH)_2$ and $(DCOOH)_2$ in rare gas matrices: a comparative study with gas phase spectra. J Chem Phys 128(11):114310
19. Olbert-Majkut A, Ahokas J, Lundell J, Pettersson M (2009) Raman spectroscopy of formic acid and its dimers isolated in low temperature argon matrices. Chem Phys Lett 468(4):176–183
20. Marushkevich K, Khriachtchev L, Lundell J, Domanskaya A, Räsänen M (2010) Matrix isolation and ab initio study of trans–trans and trans–cis dimers of formic acid. J Phys Chem A 114(10):3495–3502
21. Ito F (2015) Infrared spectra of formic acid clusters in noble gas matrices. J Mol Struct 1091:203–209
22. Lopes S, Fausto R, Khriachtchev L (2018) Formic acid dimers in a nitrogen matrix. J Chem Phys 148(3):034301
23. Ito F (2010) Modeling and spectral simulation of matrix-isolated molecules by density functional calculations: a case study on formic acid dimer. J Chem Phys 133(21):214502
24. Ito F (2019) Modeling and spectral simulation of formic acid dimer in Ar matrix using ONIOM calculations. Comput Theor Chem 1161:18–25
25. von Puttkamer K, Quack M (1987) High resolution interferometric FTIR spectroscopy of $(HF)_2$: analysis of a low frequency fundamental near 400 cm^{-1}. Mol Phys 62(5):1047–1064
26. Xue Z, Suhm MA (2009) Probing the stiffness of the simplest double hydrogen bond: the symmetric hydrogen bond modes of jet-cooled formic acid dimer. J Chem Phys 131(5):054301
27. Chocholoušová J, Vacek J, Hobza P (2002) Potential energy and free energy surfaces of the formic acid dimer: correlated ab initio calculations and molecular dynamics simulations. Phys Chem Chem Phys 4:2119–2122
28. Roszak S, Gee RH, Balasubramanian K, Fried LE (2005) New theoretical insight into the interactions and properties of formic acid: development of a quantum-based pair potential for formic acid. J Chem Phys 123(14):144702
29. Miliordos E, Xantheas SS (2015) On the validity of the basis set superposition error and complete basis set limit extrapolations for the binding energy of the formic acid dimer. J Chem Phys 142(9):094311
30. Barnes GL, Sibert EL III (2008) The effects of asymmetric motions on the tunneling splittings in formic acid dimer. J Chem Phys 129(16):164317
31. Chen Q, Bowman JM (2016) An ab initio potential energy surface for the formic acid dimer: zero-point energy, selected anharmonic fundamental energies, and ground-state tunneling splitting calculated in relaxed 1−4-mode subspaces. Phys Chem Chem Phys 18:24835–24840
32. Millikan RC, Pitzer KS (1958) The infrared spectra of dimeric and crystalline formic acid. J Am Chem Soc 80(14):3515–3521
33. Hirota K, Nakai Y (1959) Far infrared spectrum of gaseous formic acid. Bull Chem Soc Jpn 32(7):769–771

34. Dunning TH (1989) Gaussian basis sets for use in correlated molecular calculations. I. The atoms boron through neon and hydrogen. J Chem Phys 90(2):1007–1023
35. Kendall RA, Dunning TH, Harrison RJ (1992) Electron affinities of the first-row atoms revisited. Systematic basis sets and wave functions. J Chem Phys 96(9):6796–6806
36. Florio GM, Zwier TS, Myshakin EM, Jordan KD, Sibert EL III (2003) Theoretical modeling of the OH stretch infrared spectrum of carboxylic acid dimers based on first-principles anharmonic couplings. J Chem Phys 118(4):1735–1746
37. Kalescky R, Kraka E, Cremer D (2014) Accurate determination of the binding energy of the formic acid dimer: the importance of geometry relaxation. J Chem Phys 140(8):084315
38. Heger M, Suhm MA, Mata RA (2014) Communication: towards the binding energy and vibrational red shift of the simplest organic hydrogen bond: Harmonic constraints for methanol dimer. J Chem Phys 141(10):101105
39. Chen Q, Bowman JM (2019) Quantum approaches to vibrational dynamics and spectroscopy: is ease of interpretation sacrificed as rigor increases? Phys Chem Chem Phys 21:3397–3413
40. Barone V (2005) Anharmonic vibrational properties by a fully automated second-order perturbative approach. J Chem Phys 122(1):014108
41. Häber T, Schmitt U, Emmeluth C, Suhm MA (2001) Ragout-jet FTIR spectroscopy of cluster isomerism and cluster dynamics: from carboxylic acid dimers to N_2O nanoparticles. Faraday Discuss 118:331–359
42. Matanović I, Došlić N (2007) Theoretical modeling of the formic acid dimer infrared spectrum: shaping the O–H stretch band. Chem Phys 338(2):121–126
43. Barone V, Biczysko M, Bloino J (2014) Fully anharmonic IR and Raman spectra of medium-size molecular systems: accuracy and interpretation. Phys Chem Chem Phys 16:1759–1787
44. Pitsevich GA, Malevich AE, Kozlovskaya EN, Doroshenko IY, Sablinskas V, Pogorelov VE, Dovgal D, Balevicius V (2015) Anharmonic analysis of CH and OH stretching vibrations of the formic acid dimer. Vib Spectrosc 79:67–75
45. Yavuz İ, Trindle C (2008) Structure, binding energies, and IR-spectral fingerprinting of formic acid dimers. J Chem Theory Comput 4(3):533–541
46. Meyer KAE, Suhm MA (2019) Stretching of *cis*-formic acid: warm-up and cool-down as molecular work-out. Chem Sci 10:6285–6294
47. Chen Q, Bowman JM (2018) IR spectra of $(HCOOH)_2$ and $(DCOOH)_2$: experiment, VSCF/VCI, and ab initio molecular dynamics calculations using full-dimensional potential and dipole moment surfaces. J Phys Chem Lett 9(10):2604–2610
48. Bowman JM, Carrington T, Meyer HD (2008) Variational quantum approaches for computing vibrational energies of polyatomic molecules. Mol Phys 106(16–18):2145–2182
49. Császár AG, Fábri C, Szidarovszky T, Mátyus E, Furtenbacher T, Czakó G (2012) The fourth age of quantum chemistry: molecules in motion. Phys Chem Chem Phys 14:1085–1106
50. Mackeprang K, Zhen-Hao X, Maroun Z, Meuwly M, Kjaergaard HG (2016) Spectroscopy and dynamics of double proton transfer in formic acid dimer. Phys Chem Chem Phys 18:24654–24662
51. Thomas M, Brehm M, Fligg R, Vähringer P, Kirchner B (2013) Computing vibrational spectra from ab initio molecular dynamics. Phys Chem Chem Phys 15:6608–6622
52. Madeja F, Havenith M (2002) High resolution spectroscopy of carboxylic acid in the gas phase: observation of proton transfer in $(DCOOH)_2$. J Chem Phys 117(15):7162–7168
53. Luckhaus D (2006) Concerted hydrogen exchange tunneling in formic acid dimer. J Phys Chem A 110(9):3151–3158
54. Graf F, Meyer R, Ha TK, Ernst RR (1981) Dynamics of hydrogen bond exchange in carboxylic acid dimers. J Chem Phys 75(6):2914–2918
55. Chang YT, Yamaguchi Y, Miller WH, Schaefer HF III (1987) An analysis of the infrared and Raman spectra of the formic acid dimer $(HCOOH)_2$. J Am Chem Soc 109(24):7245–7253
56. Shida N, Barbara PF, Almlöf J (1991) A reaction surface Hamiltonian treatment of the double proton transfer of formic acid dimer. J Chem Phys 94(5):3633–3643
57. Loerting T, Liedl KR (1998) Toward elimination of discrepancies between theory and experiment: double proton transfer in dimers of carboxylic acids. J Am Chem Soc 120(48):12595–12600
58. Tautermann CS, Voegele AF, Liedl KR (2004) The ground-state tunneling splitting of various carboxylic acid dimers. J Chem Phys 120(2):631–637
59. Luckhaus D (2010) Hydrogen exchange in formic acid dimer: tunnelling above the barrier. Phys Chem Chem Phys 12:8357–8361
60. Mil'nikov GV, Kühn O, Nakamura H (2005) Ground-state and vibrationally assisted tunneling in the formic acid dimer. J Chem Phys 123(7):074308
61. Mil'nikov G, Nakamura H (2008) Tunneling splitting and decay of metastable states in polyatomic molecules: invariant instanton theory. Phys Chem Chem Phys 10:1374–1393
62. Matanović I, Došlić N, Kühn O (2007) Ground and asymmetric CO-stretch excited state tunneling splittings in the formic acid dimer. J Chem Phys 127(1):014309

63. Matanović I, Došlić N, Johnson BR (2008) Generalized approximation to the reaction path: the formic acid dimer case. J Chem Phys 128(8):084103
64. Mališ M, Matanović I, Došlić N (2009) A computational study of electronic and spectroscopic properties of formic acid dimer isotopologues. J Phys Chem A 113(20):6034–6040
65. Barnes GL, Squires SM, Sibert EL III (2008) Symmetric double proton tunneling in formic acid dimer: a diabatic basis approach. J Phys Chem B 112(2):595–603
66. Jain A, Sibert EL III (2015) Tunneling splittings in formic acid dimer: an adiabatic approximation to the Herring formula. J Chem Phys 142(8):084115
67. Vener MV, Kühn O, Bowman JM (2001) Vibrational spectrum of the formic acid dimer in the OH stretch region. A model 3D study. Chem Phys Lett 349(5):562–570
68. Smedarchina Z, Fernandez-Ramos A, Siebrand W (2004) Calculation of the tunneling splitting in the zero-point level and CO-stretch fundamental of the formic acid dimer. Chem Phys Lett 395(4):339–345
69. Smedarchina Z, Fernández-Ramos A, Siebrand W (2005) Tunneling dynamics of double proton transfer in formic acid and benzoic acid dimers. J Chem Phys 122(13):134309
70. Siebrand W, Smedarchina Z, Fernández-Ramos A (2008) Tunneling splitting and level ordering in a CO-stretch fundamental of the formic acid dimer. Chem Phys Lett 459(1):22–26
71. Smedarchina Z, Siebrand W, Fernández-Ramos A (2013) Zero-point tunneling splittings in compounds with multiple hydrogen bonds calculated by the rainbow instanton method. J Phys Chem A 117(43):11086–11100
72. Ivanov SD, Grant IM, Marx D (2015) Quantum free energy landscapes from ab initio path integral metadynamics: double proton transfer in the formic acid dimer is concerted but not correlated. J Chem Phys 143(12):124304
73. Richardson JO (2017) Full- and reduced-dimensionality instanton calculations of the tunnelling splitting in the formic acid dimer. Phys Chem Chem Phys 19:966–970
74. Li W, Evangelisti L, Gou Q, Caminati W, Meyer R (2019) The barrier to proton transfer in the dimer of formic acid: a pure rotational study. Angew Chem Int Ed 58(3):859–865
75. Ortlieb M, Havenith M (2007) Proton transfer in $(HCOOH)_2$: an IR high-resolution spectroscopic study of the antisymmetric C–O stretch. J Phys Chem A 111(31):7355–7363
76. Birer Ö, Havenith M (2009) High-resolution infrared spectroscopy of the formic acid dimer. Annu Rev Phys Chem 60(1):263–275
77. Goroya KG, Zhu Y, Sun P, Duan C (2014) High resolution jet-cooled infrared absorption spectra of the formic acid dimer: a reinvestigation of the C–O stretch region. J Chem Phys 140(16):164311
78. Zhang Y, Li W, Luo W, Zhu Y, Duan C (2017) High resolution jet-cooled infrared absorption spectra of $(HCOOH)_2$, $(HCOOD)_2$, and HCOOH–HCOOD complexes in 7.2 μm region. J Chem Phys 146(24):244306
79. Shipman ST, Douglass PC, Yoo HS, Hinkle CE, Mierzejewski EL, Pate BH (2007) Vibrational dynamics of carboxylic acid dimers in gas and dilute solution. Phys Chem Chem Phys 9:4572–4586
80. Bertie JE, Michaelian KH, Eysel HH, Hager D (1986) The Raman-active O–H and O–D stretching vibrations and Raman spectra of gaseous formic acid-d_1 and -OD. J Chem Phys 85(9):4779–4789
81. Meyer KAE, Suhm MA (2017) Formic acid aggregation in 2D supersonic expansions probed by FTIR imaging. J Chem Phys 147(14):144305
82. Ito F, Nakanaga T (2000) A jet-cooled infrared spectrum of the formic acid dimer by cavity ring-down spectroscopy. Chem Phys Lett 318(6):571–577
83. Ito F, Nakanaga T (2002) Jet-cooled infrared spectra of the formic acid dimer by cavity ring-down spectroscopy: observation of the O–H stretching region. Chem Phys 277(2):163–169
84. Yoon YH, Hause ML, Case AS, Crim FF (2008) Vibrational action spectroscopy of the C–H and C–D stretches in partially deuterated formic acid dimer. J Chem Phys 128(8):084305
85. Heyne K, Huse N, Dreyer J, Nibbering ETJ, Elsaesser T, Mukamel S (2004) Coherent low-frequency motions of hydrogen bonded acetic acid dimers in the liquid phase. J Chem Phys 121(2):902–913
86. Sobyra TB, Melvin MP, Nathanson GM (2017) Liquid microjet measurements of the entry of organic acids and bases into salty water. J Phys Chem C 121(38):20911–20924
87. Thomas DA, Marianski M, Mucha E, Meijer G, Johnson MA, von Helden G (2018) Ground-state structure of the proton-bound formate dimer by cold-ion infrared action spectroscopy. Angew Chem Int Ed 57(33):10615–10619
88. Davies JA, Hanson-Heine MWD, Besley NA, Shirley A, Trowers J, Yang S, Ellis AM (2019) Dimers of acetic acid in helium nanodroplets. Phys Chem Chem Phys 21:13950–13958
89. Giubertoni G, Sofronov OO, Bakker HJ (2019) Observation of distinct carboxylic acid conformers in aqueous solution. J Phys Chem Lett 10(12):3217–3222
90. Tew DP, Mizukami W (2016) Ab initio vibrational spectroscopy of *cis*- and *trans*-formic acid from a global potential energy surface. J Phys Chem A 120(49):9815–9828
91. Richter F, Carbonnière P (2018) Vibrational treatment of the formic acid double minimum case in valence coordinates. J Chem Phys 148(6):064303

92. Changala PB, Baraban JH (2016) Ab initio effective rotational and rovibrational Hamiltonians for non-rigid systems via curvilinear second order vibrational Møller-Plesset perturbation theory. J Chem Phys 145(17):174106
93. Carrington T (2017) Perspective: computing (ro-) vibrational spectra of molecules with more than four atoms. J Chem Phys 146(12):120902
94. Harabuchi Y, Tani R, De Silva N, Njegic B, Gordon MS, Taketsugu T (2019) Anharmonic vibrational computations with a quartic force field for curvilinear coordinates. J Chem Phys 151(6):064104
95. Maréchal Y (1987) IR spectra of carboxylic acids in the gas phase: a quantitative reinvestigation. J Chem Phys 87(11):6344–6353
96. Oswald S, Meyer E, Suhm MA (2018) Dinitrogen as a sensor for metastable carboxylic acid dimers and a weak hydrogen bond benchmarking tool. J Phys Chem A 122(11):2933–2946
97. Barnes GL, Sibert EL III (2008) Elucidating energy disposal pathways following excitation of the symmetric OH stretching band in formic acid dimer. Chem Phys Lett 460(1):42–45
98. Brinkmann NR, Tschumper GS, Yan G, Schaefer HF III (2003) An alternative mechanism for the dimerization of formic acid. J Phys Chem A 107(47):10208–10216
99. Madeja F, Havenith M, Nauta K, Miller RE, Chocholoušová J, Hobza P (2004) Polar isomer of formic acid dimers formed in helium nanodroplets. J Chem Phys 120(22):10554–10560
100. Rodziewicz P, Doltsinis NL (2009) Formic acid dimerization: evidence for species diversity from first principles simulations. J Phys Chem A 113(22):6266–6274
101. Balabin RM (2009) Polar (acyclic) isomer of formic acid dimer: gas-phase raman spectroscopy study and thermodynamic parameters. J Phys Chem A 113(17):4910–4918
102. Marushkevich K, Khriachtchev L, Räsänen M, Melavuori M, Lundell J (2012) Dimers of the higher-energy conformer of formic acid: experimental observation. J Phys Chem A 116(9):2101–2108
103. Farfán P, Echeverri A, Diaz E, Tapia JD, Gómez S, Restrepo A (2017) Dimers of formic acid: structures, stability, and double proton transfer. J Chem Phys 147(4):044312
104. Marushkevich K, Siltanen M, Räsänen M, Halonen L, Khriachtchev L (2011) Identification of new dimers of formic acid: the use of a continuous-wave optical parametric oscillator in matrix isolation experiments. J Phys Chem Lett 2(7):695–699
105. Okrasiński P, Latajka Z, Hättig C (2014) Theoretical study on noncovalent interactions in the carbon nanotube-formic acid dimer system. J Phys Chem C 118(8):4483–4488
106. Chen Q, Bowman JM (2018) High-dimensional fitting of sparse datasets of CCSD(T) electronic energies and MP2 dipole moments, illustrated for the formic acid dimer and its complex IR spectrum. J Chem Phys 148(24):241713
107. Dubecký M, Jurečka P, Mitas L, Ditte M, Fanta R (2019) Toward accurate hydrogen bonds by scalable quantum Monte Carlo. J Chem Theory Comput 15(6):3552–3557
108. Stanton JF, Gauss J, Cheng L, Harding ME, Matthews DA, Szalay PG: CFOUR, coupled-cluster techniques for computational chemistry, a quantum-chemical program package. For the current version. http://www.cfour.de
109. Frisch MJ et al (2009) Gaussian 09 Revision E.01. Gaussian Inc. Wallingford CT
110. Chemcraft—graphical software for visualization of quantum chemistry computations. https://www.chemcraftprog.com
111. Hunter JD (2007) Matplotlib: a 2D graphics environment. Comput Sci Eng 9(3):90–95

Arman Nejad received his MSc in chemistry at the University of Göttingen in 2018 where he now continues his PhD studies. He completed his master thesis on anharmonic vibrational modelling of formic acid monomer under supervision of Deborah L. Crittenden in Christchurch. His research topics include spectroscopy and anharmonic modelling of formic acid monomer and dimer as model systems to disentangle error contributions from electronic treatment, PES representation and nuclear vibrational model.

Martin Suhm has been a professor of Physical Chemistry at the University of Göttingen since 1997. He is interested in weak interactions between and in molecules and in their consequences for vibrational spectra. This is particularly true for hydrogen bonds, or hydrogen bridges as they are called more neutrally in German. What counts are the observables—we all agree that a rose, by any other name, would smell as sweet. Therefore, Martin Suhm has a passion for experimental benchmarks in the field of non-covalent interactions, helping us to judge the strengths and weaknesses of different computational models in reproducing nature.